Space-Charge Effects in RF Photoinjectors

Bruce Carlsten
Los Alamos National Laboratory
April 18, 2013

Space charge in photoinjectors

High brightness electron beams belong to a significantly different space-charge community (but with many shared concepts and terms)

- Beams in RF photoinjectors are highly space-charge dominated and very quasi-laminar, and never reach a stationary state

- We care about emittance growth in this regime which will dominate beam evolution as the beam gets accelerated and enters the emittance-dominated regime

- The emittance growth arises from space-charge nonlinearities from both time-dependent (axial) and radial nonuniformities

- Much of the emittance growth is reversible – our modeling is actually very accurate (IMPACT, OPAL, PARMELA, others)

I'll mostly be talking about projected rms emittances instead of slice rms emittances although slice emittances dictate FEL performance

Outline

- Description of RF photoinjectors
- Basic space-charge induced emittance growth
- Transverse plasma oscillations and emittance oscillations
- Comparison to DC beams and radial nonuniformities
- Dominant mechanisms for final emittance
  - Wavebreaking
  - Landau damping of emittance oscillations
- Other space-charge comments

I would like to acknowledge important contributions and slides from Dinh Nguyen and Steve Russell

Schematic of an RF Photoinjector

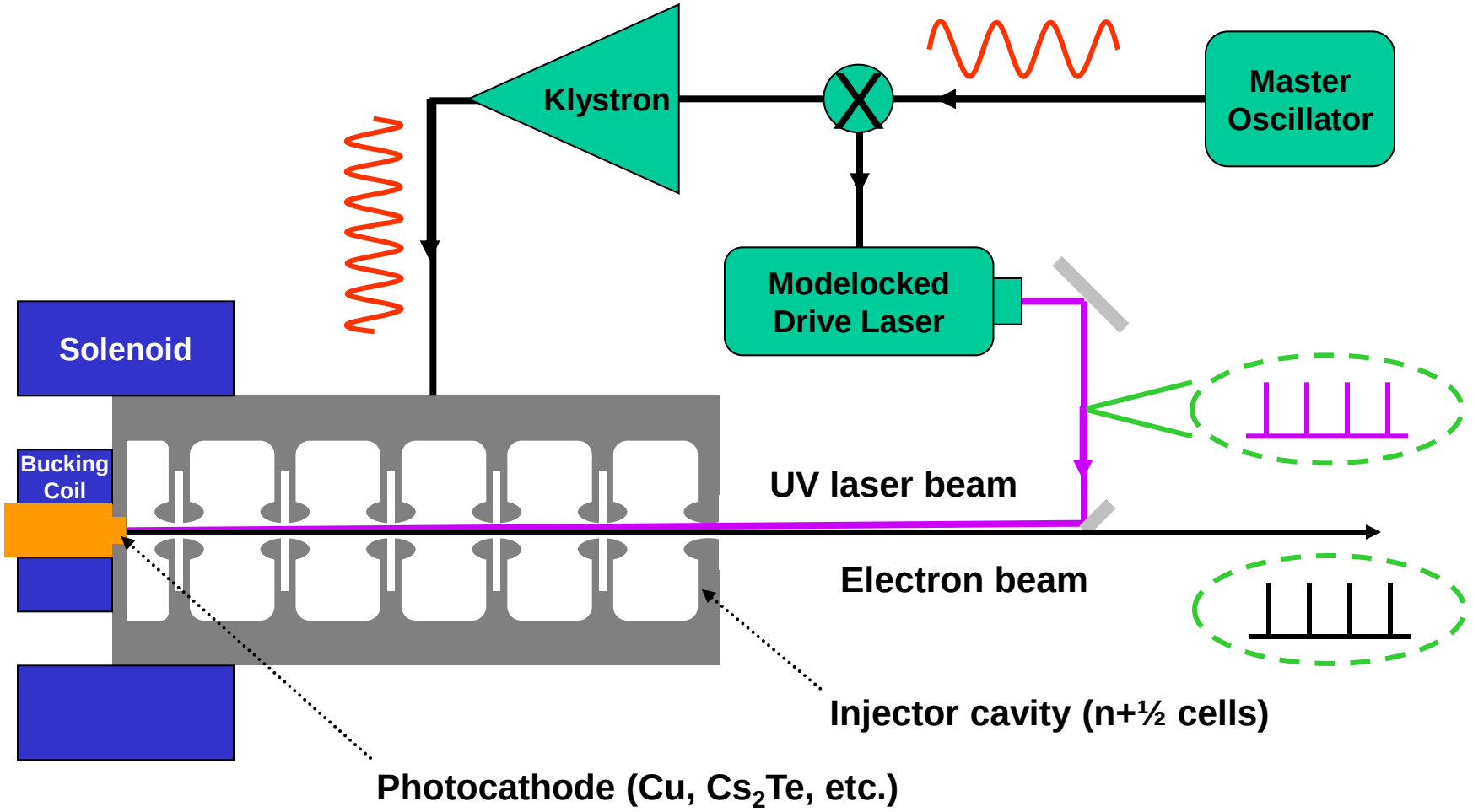

Normalized emittance for 1 nC has been reduced from tens of μm to 1 μm

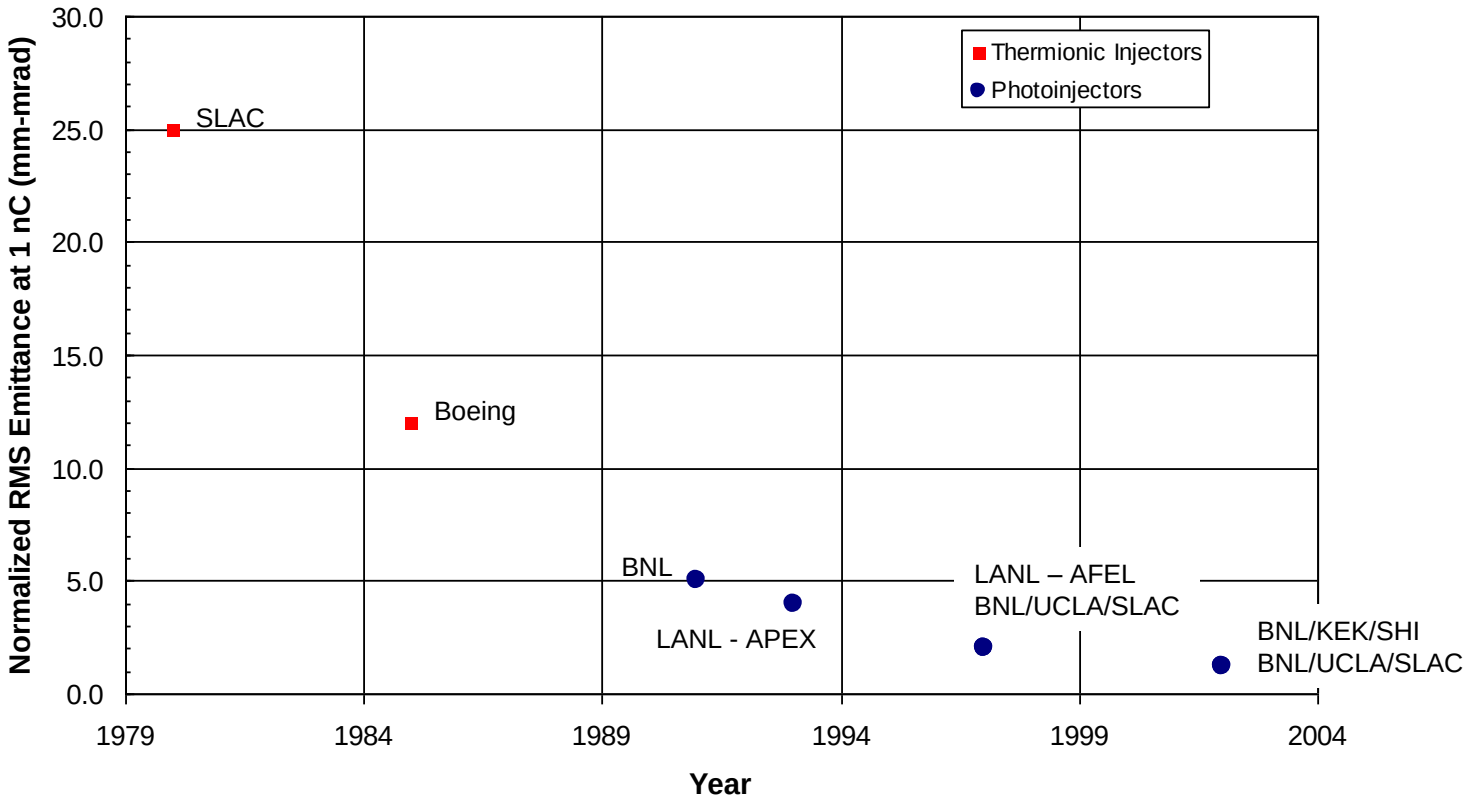

LCLS scaling: $\varepsilon_n = 1\,(\mu\text{m})\sqrt{q(\text{nC})}$

PITZ scaling: $\varepsilon_n = 0.7\,(\mu\text{m})\sqrt{q(\text{nC})}$

APEX photoinjector

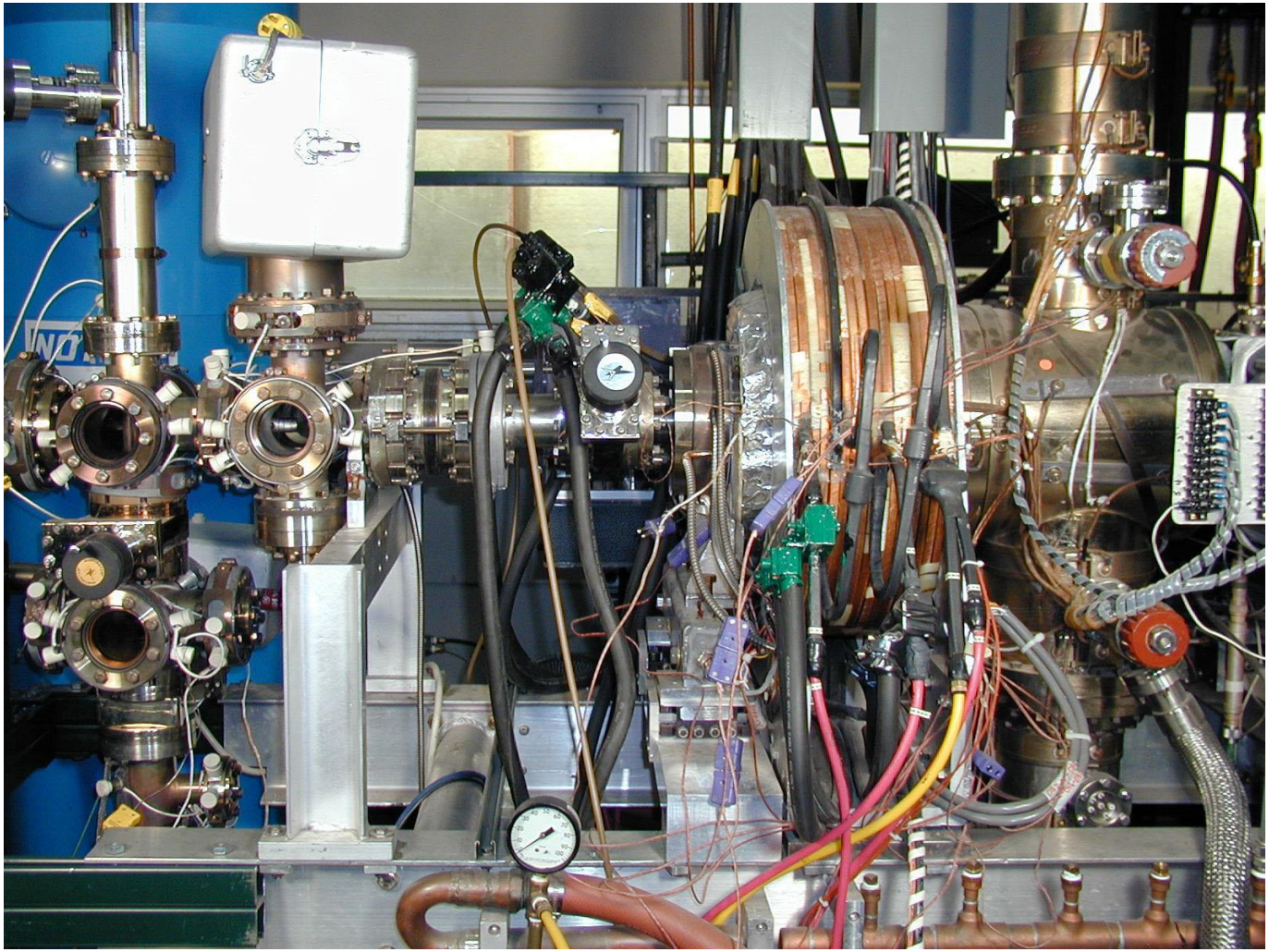

APEX photoinjector performance

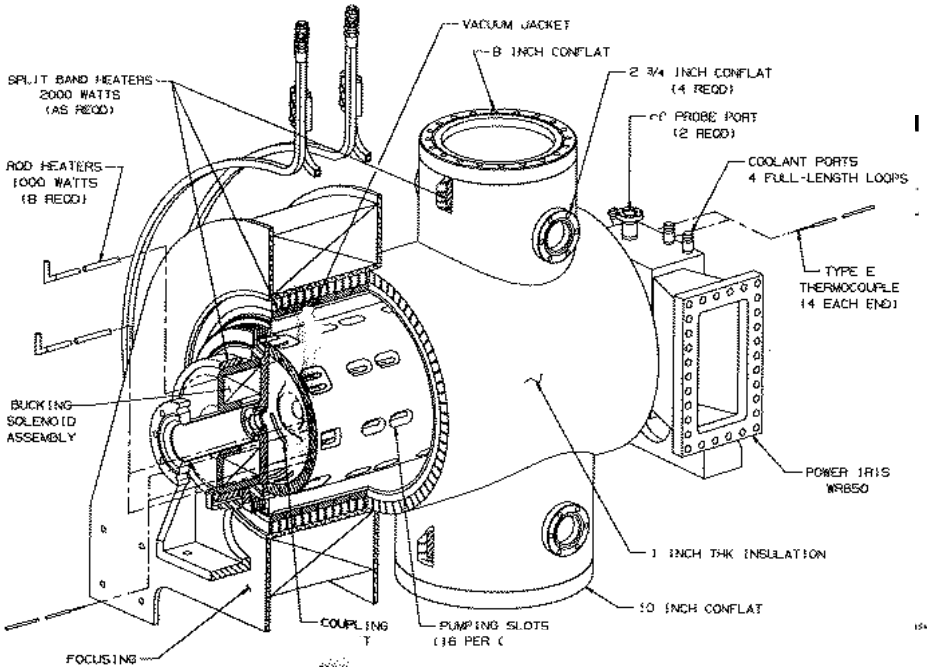

- 5 ½ cell, 1300 MHz standing wave structure.
- Output energy: 7 – 8 MeV
- Charge/bunch ≤ 10 nC

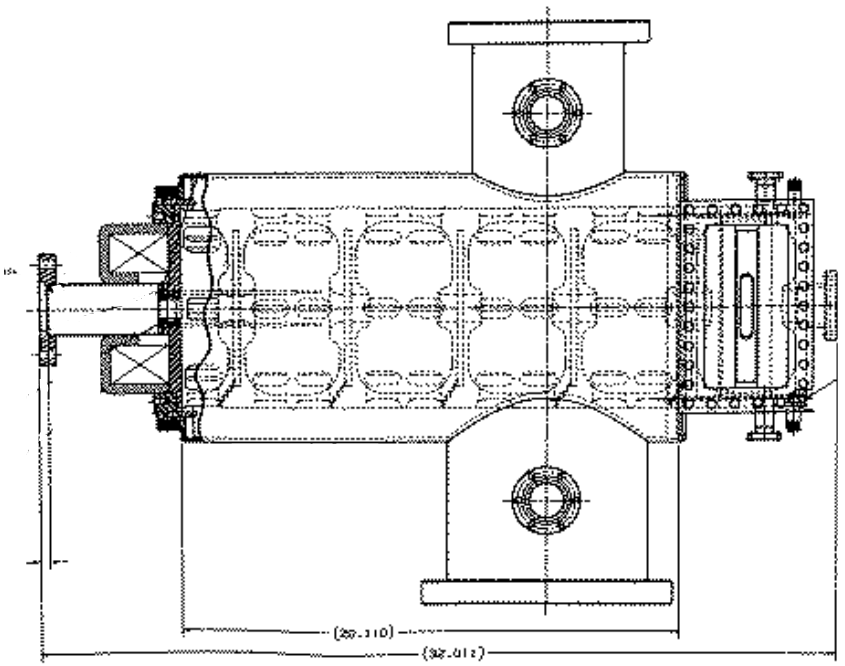

- Normalized emittance (10 ps beam):
  2.5 μm at 1 nC/bunch
  8 μm at 5 nC/bunch
- Electron bunch length: 20 ps FWHM compressed to less than 1 ps FWHM with magnetic bunching.

Typical cavity design
electric and magnetic field distribution

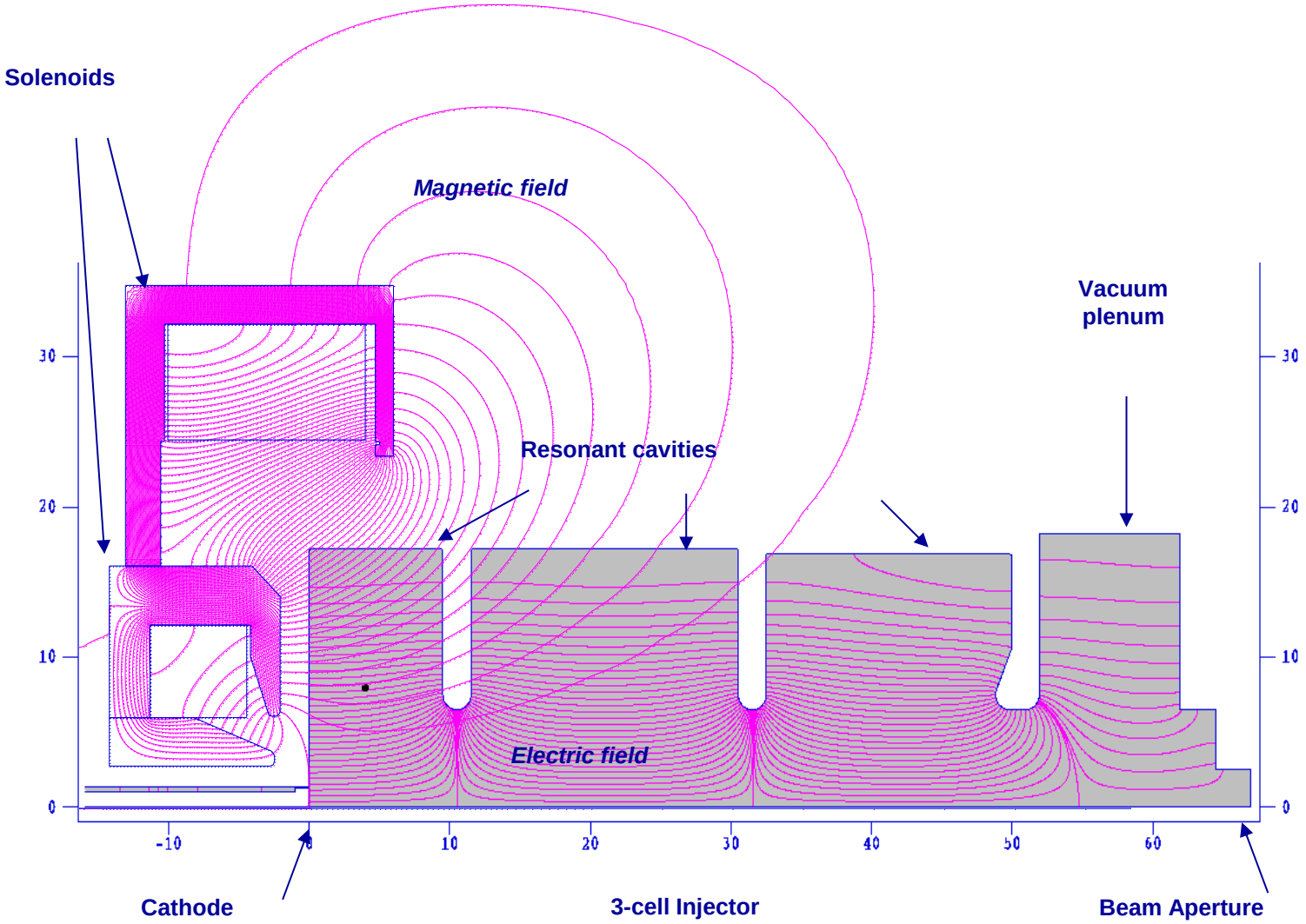

Snapshots of axial electric and magnetic fields: 30^o phase

Axial electric field

$$E_z(z,t) = E_0 \cos(kz)\sin(\omega t + \phi_0)$$

Axial magnetic field

$$B_z(z) = B_0 z^2 e^{-z}$$

Image charge

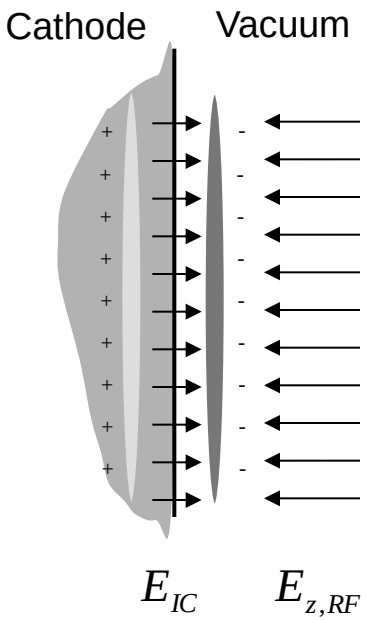

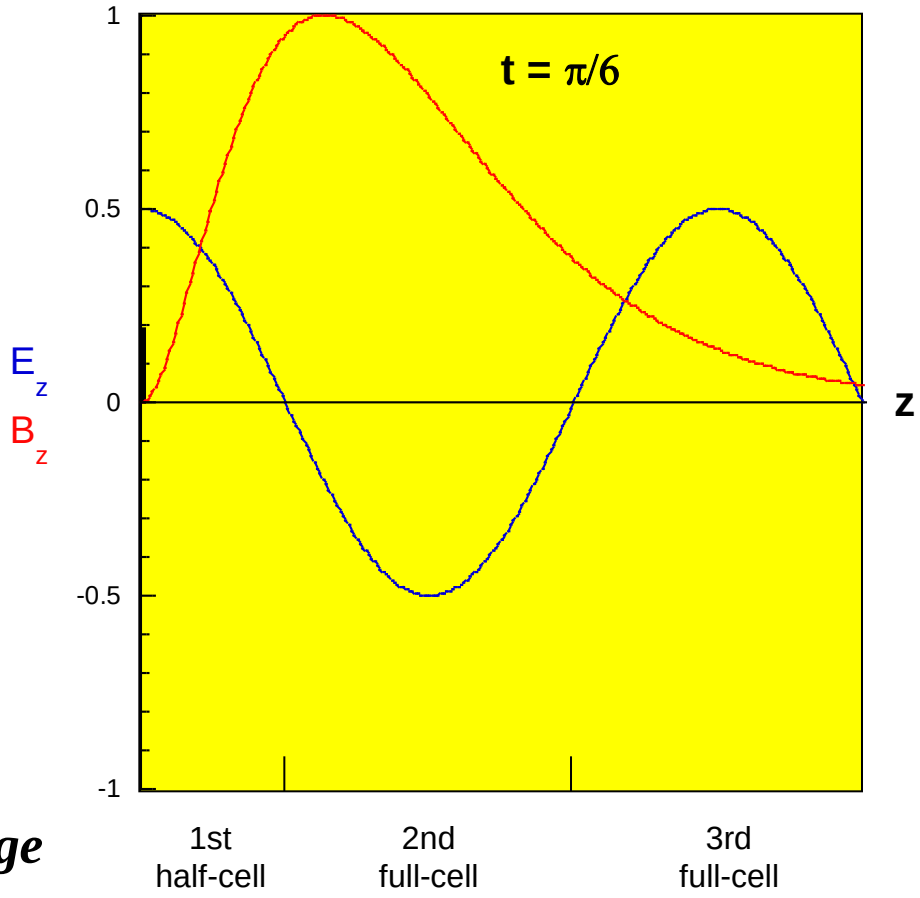

Highly nonlinear radial space-charge force

Longitudinal force

$$F_z = e\left(E_{z,RF} - E_{IC}\right)$$

$$E_{IC} = \frac{q}{\varepsilon_0 A}$$

Transverse force

$$F_r = e\left(E_r - v_z B_\theta\right)$$

$$E_r = -\frac{r}{2}\frac{\partial E_z}{\partial z} \approx 0$$

$$B_\theta = \frac{r}{2c^2}\frac{\partial E_z}{\partial t}$$

Snapshots of axial electric and magnetic fields: 60^{o} phase

Axial electric field

$$E_z(z,t) = E_0 \cos(kz)\sin(\omega t + \phi_0)$$

Axial magnetic field

$$B_z(z) = B_0 z^2 e^{-z}$$

Electron bunch length

$$F = ma$$

$$F = eE_z$$

$$\Delta z = \frac{a}{2}\left(t_1^2 - t_2^2\right)$$

$$t_1 = t$$

$$t_2 = t + \Delta t$$

$$\Delta z = \frac{eE_z t \Delta t}{m}$$

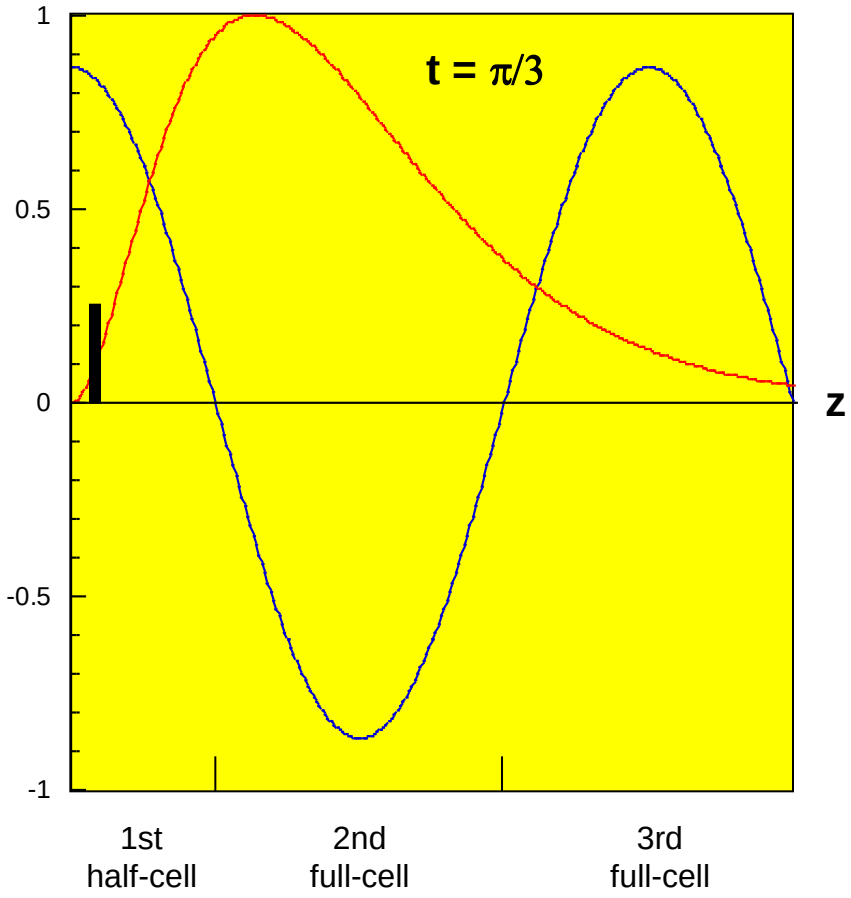

Example:

$$E_z = 20MV/m$$

$$e = 1.6\times10^{-19}\cdot C$$

$$m = 9.1\times10^{-31}\cdot kg$$

$$t = 60\cdot ps$$

$$\Delta t = 10\cdot ps$$

$$\Delta z = 2\cdot mm$$

Snapshots of axial electric and magnetic fields: 90º phase

Axial electric field

$$E_z(z,t) = E_0 \cos(kz)\sin(\omega t + \phi_0)$$

Axial magnetic field

$$B_z(z) = B_0 z^2 e^{-z}$$

Lab frame

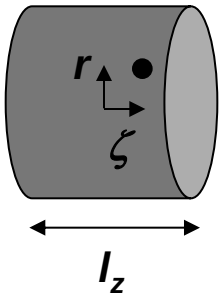

Bunch rest frame

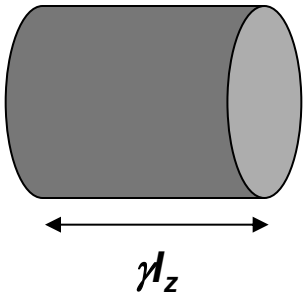

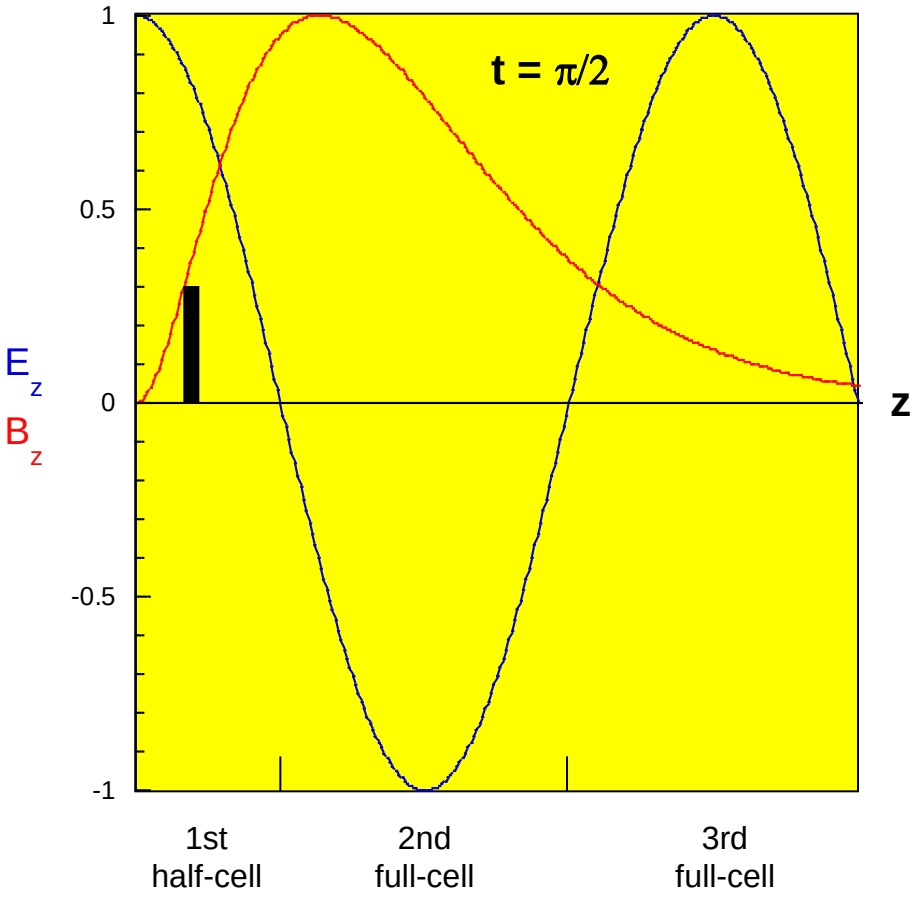

Longitudinal force

$$F_z = e\left(E_{z,RF} - E_{IC} + E_{SC}\right)$$

$$E_{z,SC} = \rho_0 f(\zeta)$$

Transverse forces

$$F_\theta = e v_r B_z$$

$$F_r = e\left(E_{r,SC} + v_\theta B_z\right)$$

$$E_{r,SC} = \rho_0 g(r,\zeta)$$

Snapshots of axial electric and magnetic fields: 120^{o} phase

Axial electric field

$$E_z(z,t) = E_0 \cos(kz)\sin(\omega t + \phi_0)$$

Axial magnetic field

$$B_z(z) = B_0 z^2 e^{-z}$$

Fields in rest frame

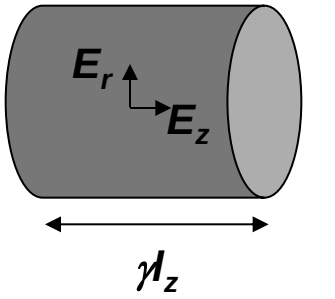

$$F'_{z,SC} \propto \frac{1}{\gamma^2}$$

$$F'_{r,SC} \propto \frac{1}{\gamma^2}$$

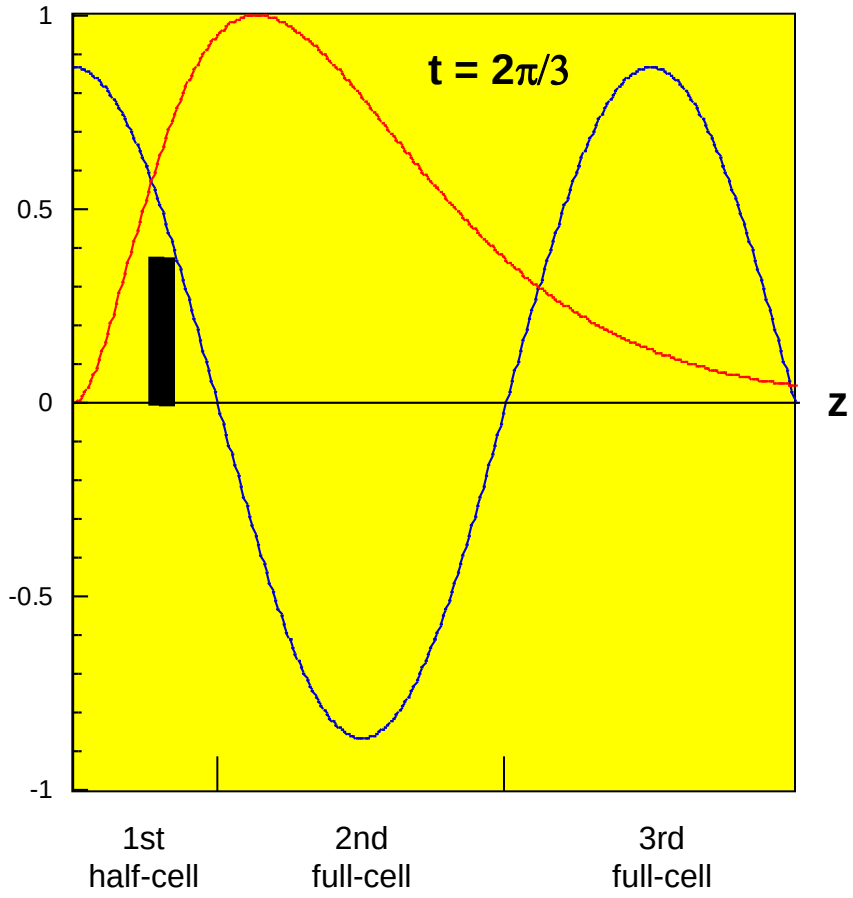

K-J Kim integrated motion in photoinjector to estimate emittance growth

These expressions are for the emittance due to time-varying (axial variations) in RF forces, space-charge forces and dominate the initial emittance growth:

$$\varepsilon_{x,RF} = \frac{\alpha k \left\langle x^2 \right\rangle}{\sqrt{2}} \sigma_\phi^2$$

$$\varepsilon_{x,sc} = \frac{\pi}{4} \frac{1}{\alpha k \sin\phi_0} \frac{I}{I_A} \frac{1}{3A+5}$$

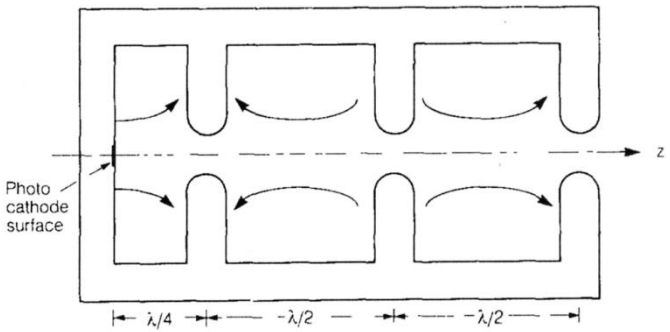

Fig. 1. Schematics of the rf laser gun.

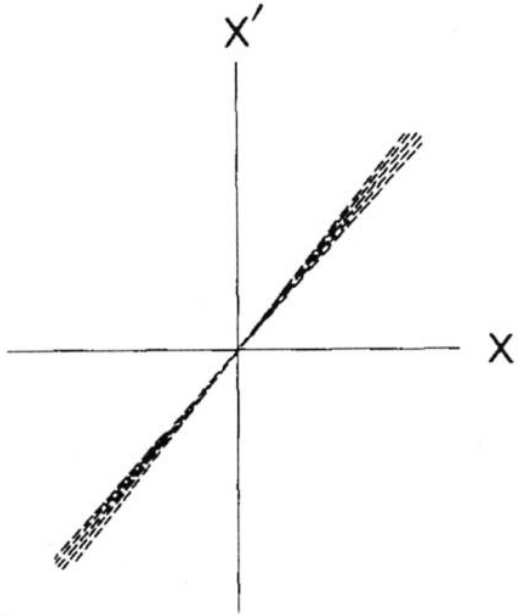

Emittance oscillations in nominal RF gun design (700 MHz, 3 nC, 9 ps)

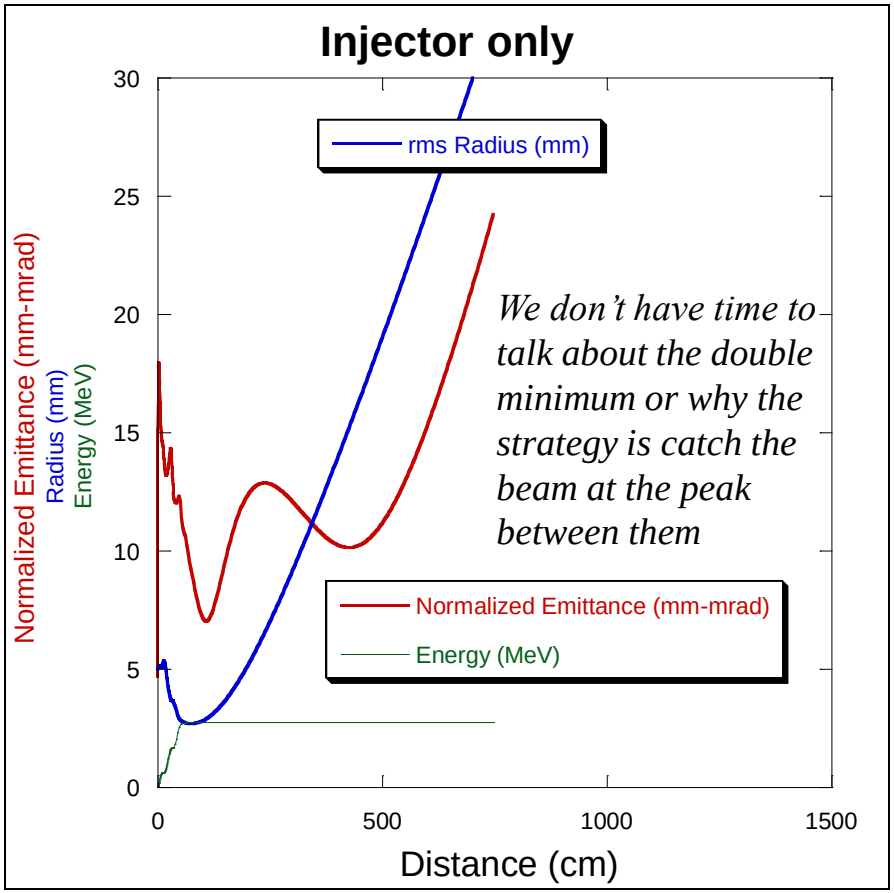

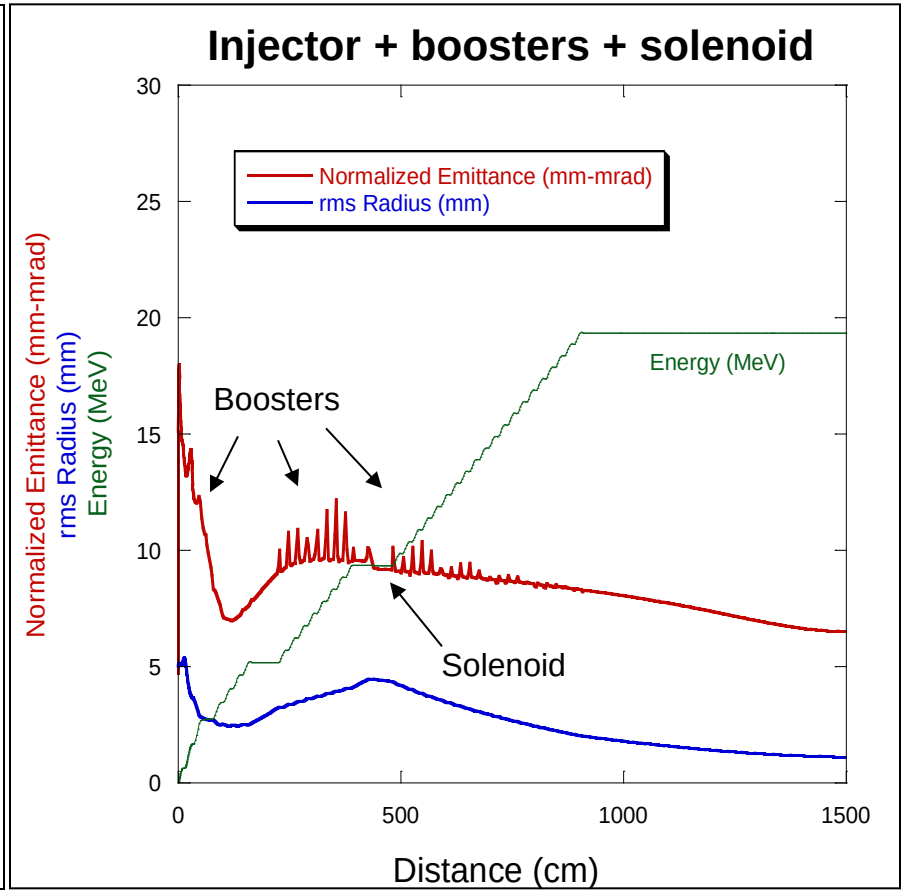

Adding booster linacs and a second solenoid allows different phase-space envelopes to realign at higher energy, resulting in a lower beam emittance

The emittance reduction is known as emittance compensation

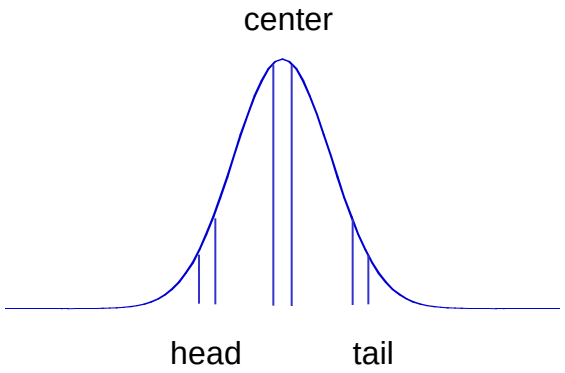

Electron bunch is sliced into N axial slices, each having its own phase space ellipse

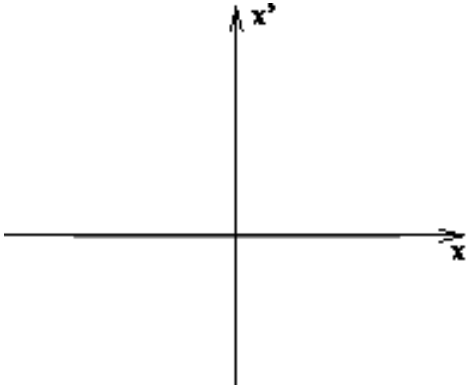

a

Initially all phase space ellipses are aligned

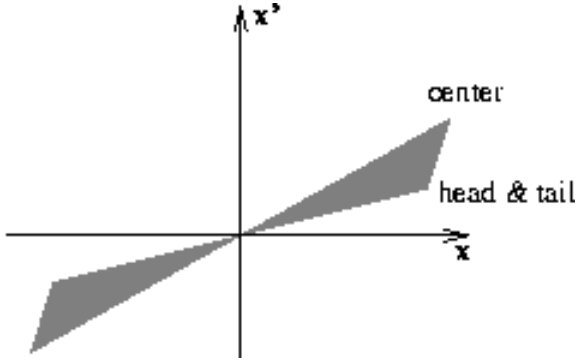

b

Space charge causes phase space ellipses to fan out, thus large projected emittance

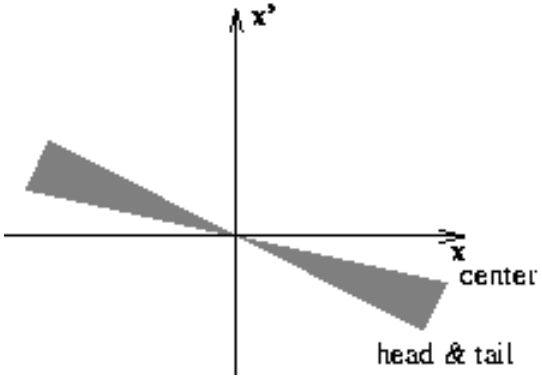

c

Magnetic solenoid acts like a lens, flipping the phase space ellipses

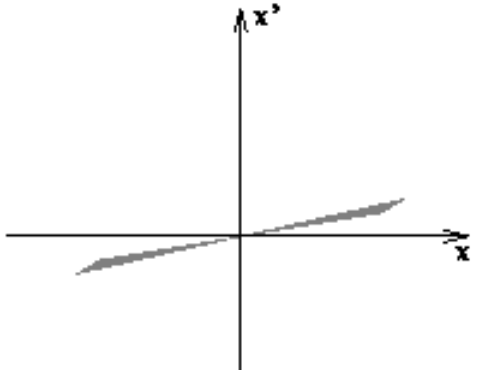

d

Different phase space ellipses realigned to yield small projected emittance

Emittance compensation modeling for a drifting slug of charge

Focusing lens at 28 cm:

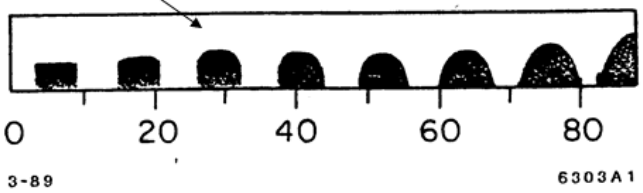

This emittance is 4 times the rms emittance

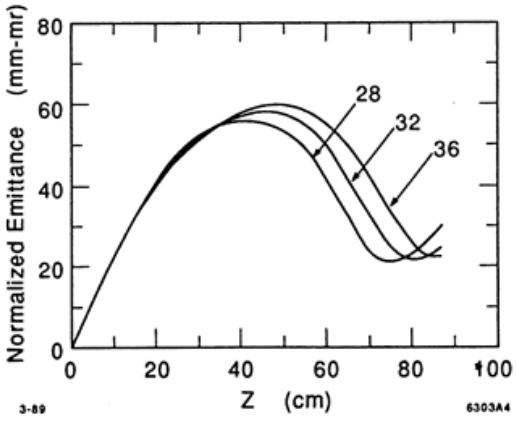

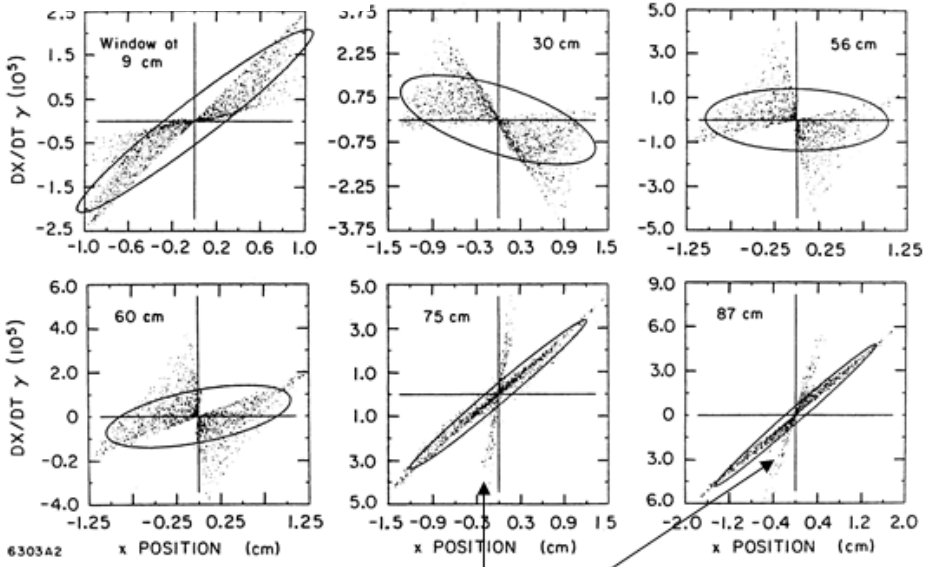

These particles dominate the final emittance – note the beam is diverging at the minimum emittance position

Emittance oscillations results from plasma oscillations

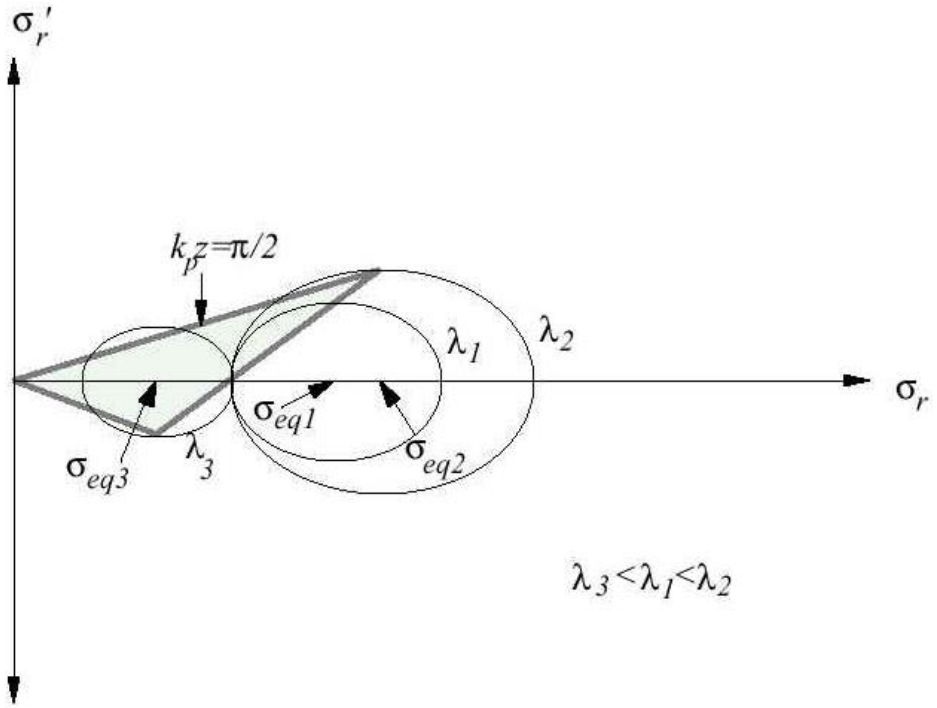

$$\sigma'' + K\sigma - K_s/\sigma = 0$$

$$K_s = 2I(r)/I_A\gamma^3\beta^3$$

$$\sigma_{eq} = \sqrt{K_s/K}$$

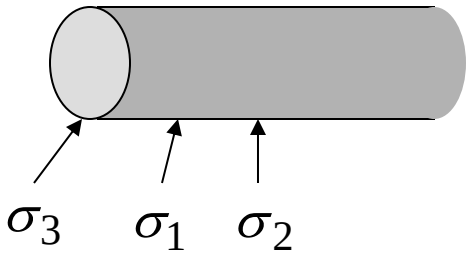

Bow-tie phase space distribution forms during the plasma oscillations of particles with different equilibrium radii

To first order, plasma oscillations all have the same period

The transverse motion of a particle in a slice of the beam in a uniform focusing channel of normalized strength *K* is given by (nonaccelerating)

$$\sigma'' + K\sigma - \frac{K_s}{\sigma} = 0$$

The equilibrium particle radius (no acceleration) is given by

$$\sigma_{eq} = \sqrt{\frac{K_s}{K}}$$

We write the particle radius as $\sigma = \delta + \sigma_{eq}$

If the beam is rms matched and the density nonuniformity is small, we get this equation:

$$\delta'' + \left(2K + K\left(\frac{\delta}{\sigma_{eq}}\right)^2\right)\delta - K\left(\frac{\delta}{\sigma_{eq}}\right)^2 \sigma_{eq} = 0$$

Nonlinear radial forces in diodes lead to radial oscillations in DC beams with the same basic physics

ρ

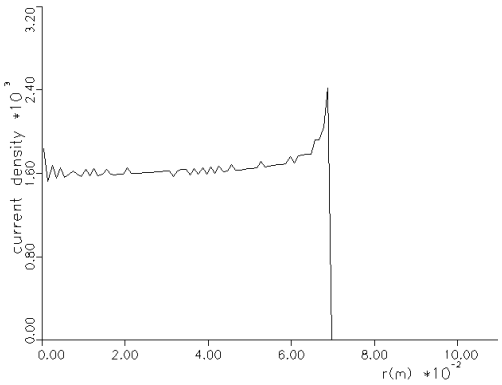

r

r'

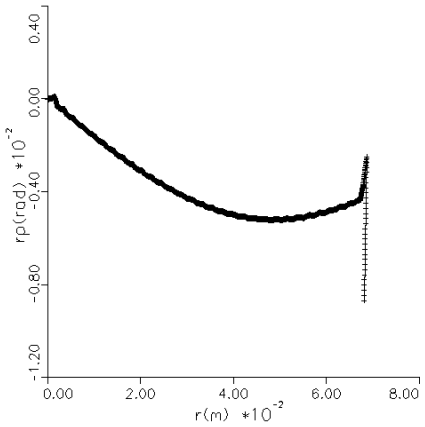

r

Nonlinear density and curvature lead to radial plasma oscillations - nonlinear potential energy effect and emittance oscillations

Also see beginnings of wavebreaking in phase space (means distribution becomes multi-valued in r)

Nominal simulation - 4 kA, 4 MeV showing emittance oscillations:

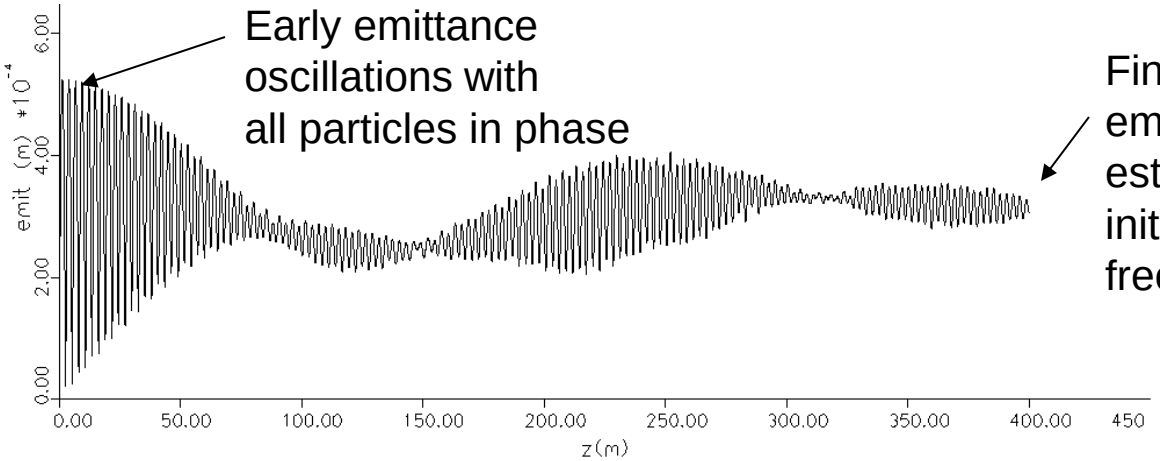

Early emittance oscillations with all particles in phase

Final thermalized emittance, can estimate from the initial nonlinear free energy

Initial radial current distribution

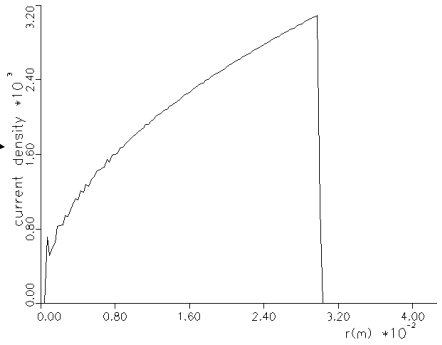

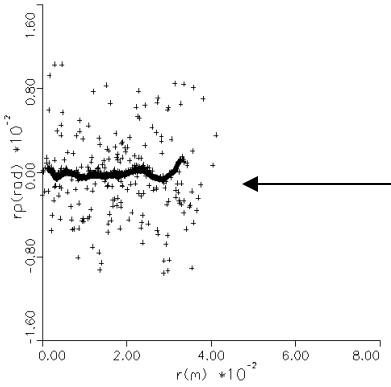

Final phase space distribution - kinks approximate final ellipse after long thermalizational

Thermalization arises from either spread in radial oscillation frequencies (Landau damping) or wavebreaking (which is suppressed in this simulation)

Wave breaking dominates final emittance for both RF photoinjectors and long DC beams

If no wave breaking occurs (in phase space), plasma oscillations will persist for very long distances before thermalization. However, if the beam wave breaks, thermalization will occur much faster with a charateristic distance of a ¼ betatron period. Large scale wave breaking (say of ½ the particles) will occur for a uniform density beam with an initial emittance exceeding

$$\varepsilon_{w-b} = 4r_e\sqrt{(I/I_A)/\gamma\beta}$$

If this happens, the initial emittance is frozen; if only a few particles wave break, they can lead to a much smaller final emittance.

High-current, high-brightness electron beams are under this limit, and do not undergo immediate, large-scale wave breaking. *However, particles with low enough density and large enough radial position will always wave break*.

Wave breaking in an RF photoinjector

Large-scale wavebreaking can occur for radially nonuniform distributions:

Uniform case - bowtie distribution results from spread in plasma frequencies

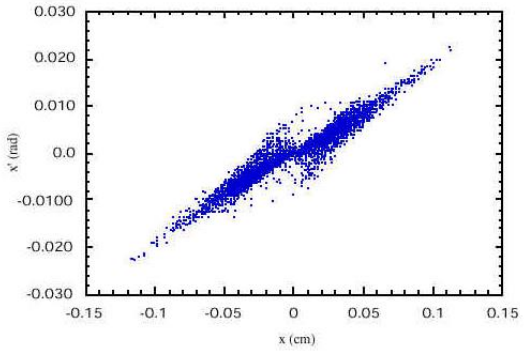

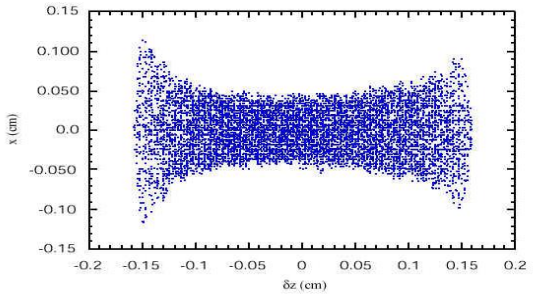

Nonuniform case - horizontal component from wavebreaking - final emittance is 4 times larger

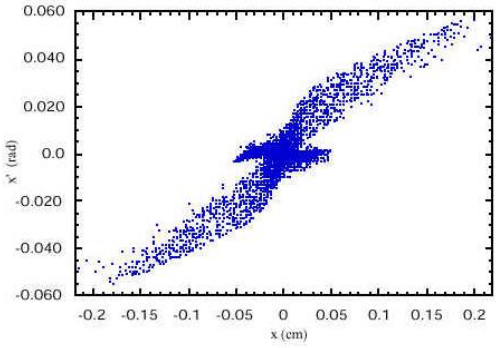

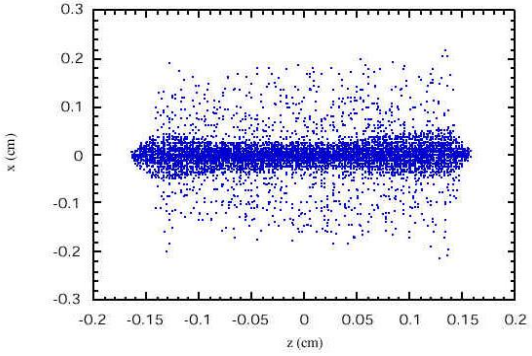

PITZ photoinjector is current state-of-the-art

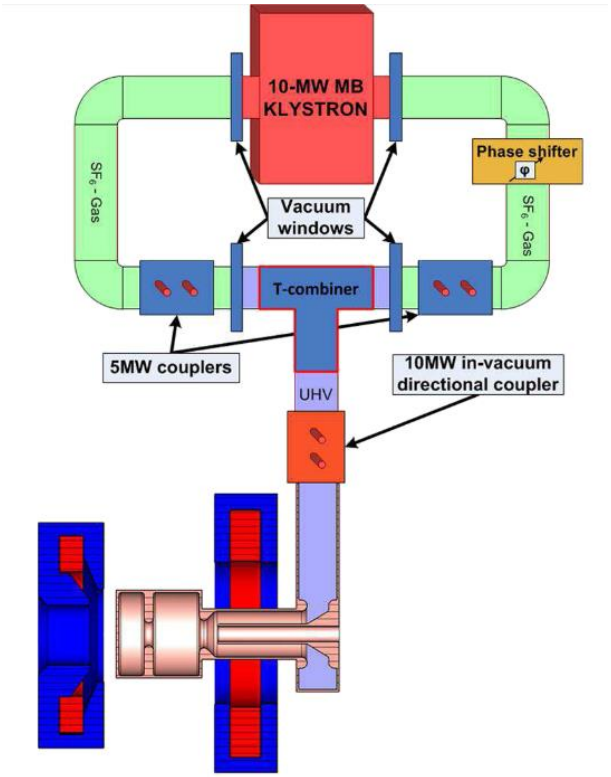

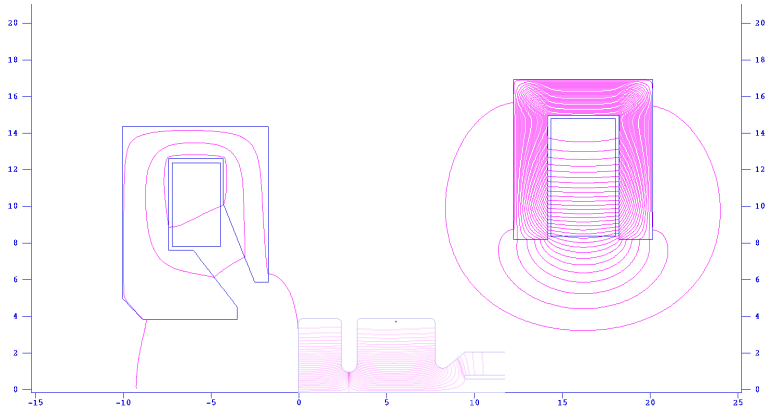

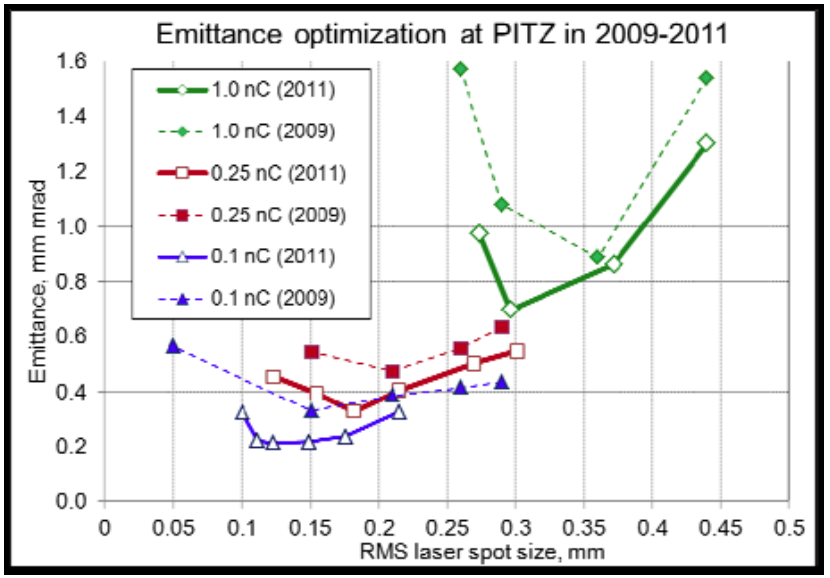

PITZ scaling:

$$\varepsilon_n = 0.7\,(\mu\mathrm{m})\sqrt{q(\mathrm{nC})}$$

MaRIE XFEL photoinjector design

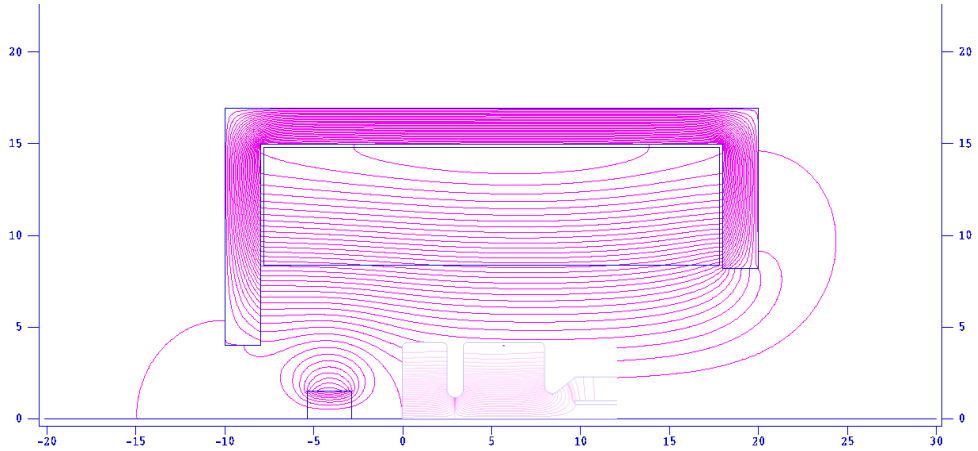

Scaled PITZ geometry (2.856 GHz), optimization of magnetic field profile allows better emittance compensation (2-way), lower amounts of wave breaking

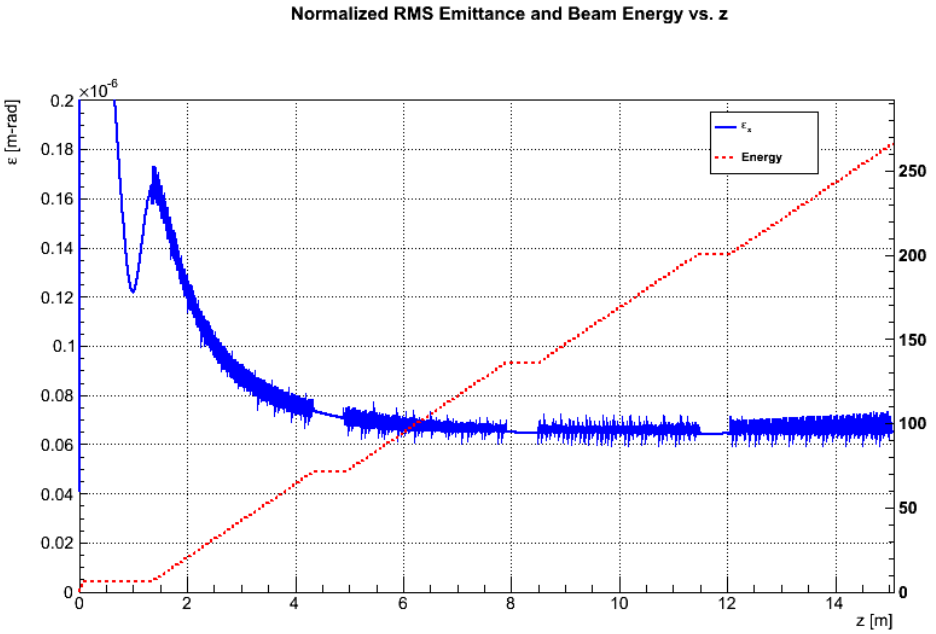

Emittance predicted to be ~ 0.1 μm for 100 pC (OPAL)

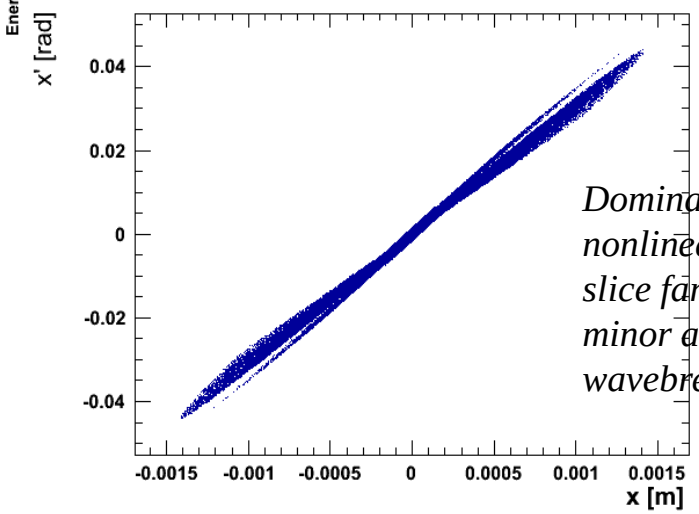

Dominated by radial nonlinearities (not slice fanning) with a minor amount of wavebreaking

MaRIE XFEL photoinjector design

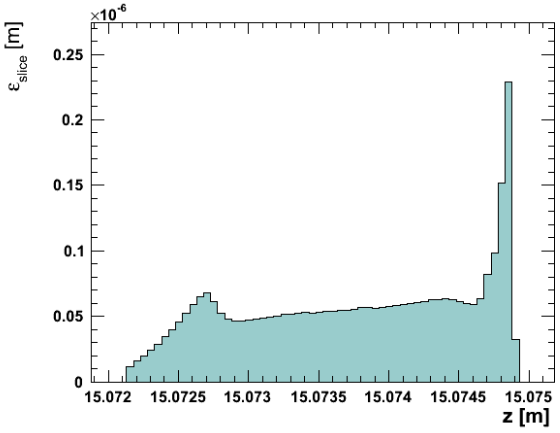

Slice emittance

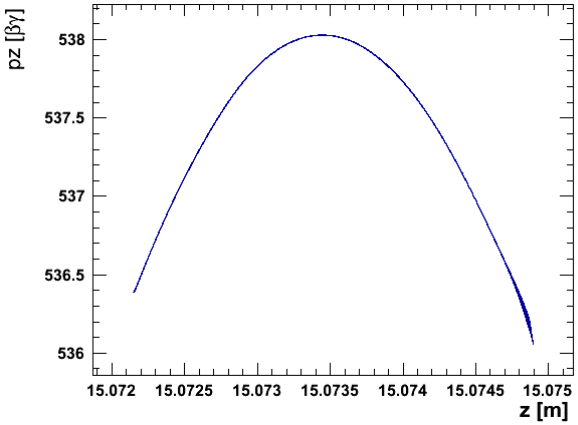

Longitudinal phase space

Beams from both RF photoinjectors and DC photo-guns (Cornell) are now reaching the thermal limits)

Property	Value
Energy	260 MeV
Charge	100 pC
Transverse ε_n	65 nm
Thermal ε_n (atomically clean copper*)	44 nm
Residual ε_n	48 nm
RMS Length	2.1 ps
RMS Energy Spread	0.08%

Current profile

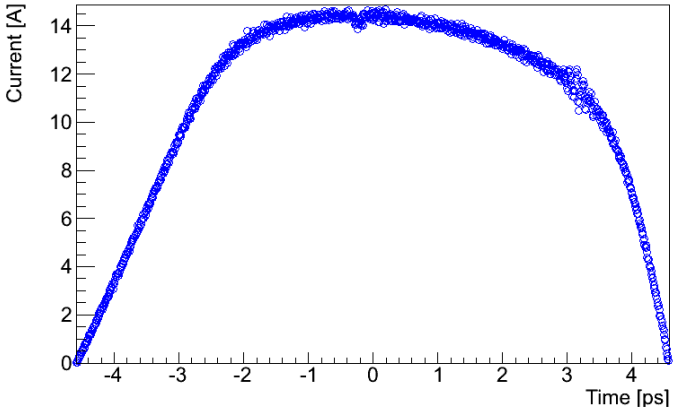

Longitudinal phase space

1. Energy spread from potential depression: $\delta\phi_{rms} = \frac{I}{48\pi\varepsilon_0\beta c}$

MaRIE photoinjector beam is very cold, with a slice RMS energy spread of about a couple hundred eV. Surprisingly, that's still above the value you'd expect from the beam's own potential depression which for 10 A is only about 25 eV.

2. The minimum longitudinal emittance for a charge Q is

$$\varepsilon_{norm,z} = \frac{Q}{48\pi\varepsilon_0 mc^2}$$

which would be about 1.5 microns for a charge of 1 nC; MaRIE photoinjector design also well above that

Summary

RF photoinjectors are becoming a mature technology.

We understand the limits of transverse emittance and are beginning to reach them (in the sense the beam is beginning to be dominated by thermal effects in modern designs). We are simultaneously compensating transverse and axial space-charge nonlinearities; residual non-thermal emittance is typically from wave-breaking due to radial effects.

Modeling photoinjectors is hard – wide range of rest frames as the beam is initiated, scattering off grid leads to artificial wave breaking

Our understanding of space-charge effects on the beam's longitudinal emittance is still immature and we should see factors of 4 or more improvements in the future. Emittance partitioning will require even greater modeling accuracy, especially for 3-D geometries. There is still a lot of work to do to understand and model coherent synchrotron radiation effects.